

AN ITERATIVE SERIES SOLUTION APPROACH FOR SOLVING THE FREE-BOUNDARY CONDITION IN GROUNDWATER FLOW SYSTEMS

Sanders Wong*, James R. Craig* and W. Wayne Read†

*Department of Civil & Environmental Engineering
University of Waterloo, Waterloo, ON, Canada
e-mail: s38wong@uwaterloo.ca, jrcraig@uwaterloo.ca
web page:<http://www.civil.uwaterloo.ca/jrcraig/>

†Department of Mathematics & Statistics
James Cook University, Townsville, QLD, Australia
e-mail: wayne.read@jcu.edu.au

Key words: Multi-layer aquifers, analytical model, series solutions, free-boundary condition;

Summary. In this paper, a two-dimensional analytic series solution for groundwater flow with a free water table condition is derived and demonstrated on a two-layer unconfined aquifer with complex (i.e., natural) stratigraphy. The vertical side and bottom boundaries of the model domain are impermeable, and the water table is a free-boundary condition governed by both Dirichlet and Neumann conditions. Unlike previous investigations, the problem is complicated by the possible intersection of the water table with interfaces between different materials. This challenge can be overcome by intelligently revising the analytic series solution approach previously developed by the authors. The series coefficients are calculated through a least-squares method which minimizes errors. Test cases are used to demonstrate the effects of both system geometry and lower aquifer conductivity upon the shape of the water table surface.

1 INTRODUCTION

The following paper addresses an amendment to the two-dimensional series solution techniques of Wong and Craig¹ whereby the water table surface is treated using a free-boundary condition (FBC) subject to a specified recharge/discharge distribution. This solution method is used to determine the influence of two factors upon the geometry of water table in a two-layer unconfined aquifer: the conductivity contrast between the layers and the geometry of the base.

2 BACKGROUND

The earliest appearance of an analytical series solution for groundwater flow is the one-layer system model of Tóth², where the topographic surface is used as the driver of regional flow in a two-dimensional rectangular region with no-flow conditions along the sides and bottom of the modeled domain. This solution was extended to an aquifer with uniform layers of different isotropic hydraulic conductivities and an arbitrary topographic surface by Freeze and Witherspoon³, though the solution was still restricted to a rectangular geometry. Recent advances in analytical series solution approaches by Read and others^{4, 5, 6, 7, 8, 9} have relaxed previous restrictions on geometry through the use of a least-squares (LS) approach. This least-squares series solution method has been applied to single-layer aquifer systems with variable elevation at the top and bottom boundaries, and later amended to handle a FBC subject to vertical recharge⁷. A similar LS approach has been developed by Craig¹⁰ to address the effects of an arbitrary number of multiple parallel or syncline layers and anisotropic layer properties. The recent model by Wong and Craig¹ extends the series solution approach to the problem of groundwater flow in a multi-layer aquifer with complex geometry, where each of the layer interfaces may be described by arbitrary functions.

While the method of Wong and Craig¹ was successfully applied to multi-layer aquifers with relatively complex geometry, the approach was still constrained by the assumption of a fixed water table, assumed to be known a priori. Here, this oversight is corrected through the use of an iterative algorithm used to identify the location of the water table when subjected to a specified recharge/discharge distribution in space. The algorithm is similar to that of Gill and Read⁷, but here used to investigate the behavior of the FBC in multilayer systems.

3 PROBLEM STATEMENT

For simplicity, the stratified aquifer is subdivided into only two layers, indexed downward from $m = 1$ to $m = 2$, each with uniform conductivity, k_m , as shown in Fig.1. The top layer is bounded by the curve $z_1(x)$ above and $z_2(x)$ below, where here the term *unconformity* is used to refer to the interface between two layers of differing hydraulic properties. The second layer is bounded by curves $z_2(x)$ and $z_b(x)$. The bottom ($z_b(x)$) and sides of the aquifer ($x = 0$ and $x = L$) are impermeable and the top of the aquifer, $z_1(x)$, is subject to the free boundary condition.

With the exception of the FBC, the problem posed is precisely that of Wong and Craig¹, and the solution may be expressed in terms of a potential function $\Phi_m = h/k_m$ in each layer. From Darcy's law and a mass balance on water, each potential function must satisfy the Laplace equation:

$$\nabla^2 \Phi^m = 0 \quad \text{for } m=1,2 \tag{1}$$

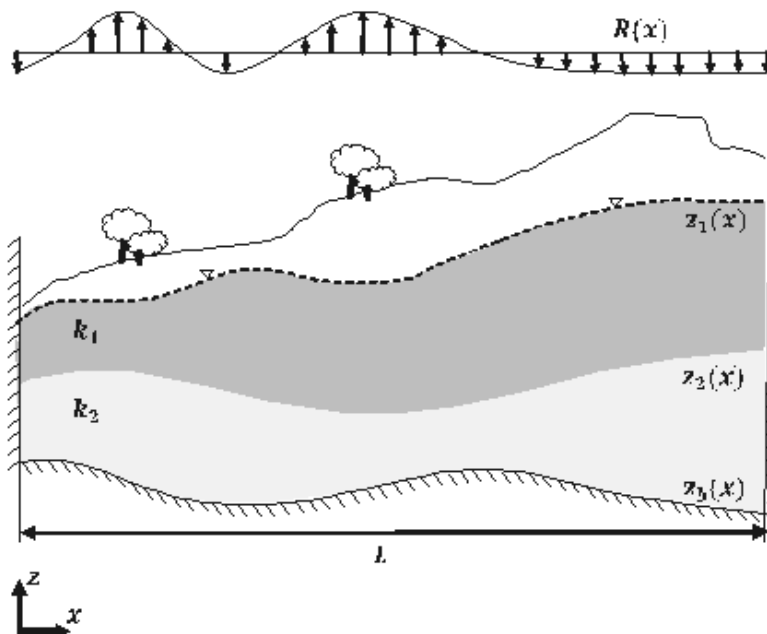


Figure 1: Layout of the general problem. Here, 2 contiguous layers are separated by the unconformities $z_2(x)$, with $z_b(x)$ corresponding to the bottom no-flow boundary and $z_1(x)$ corresponding to the top free boundary. Each layer has a unique value of hydraulic conductivity, k_m .

A normal head gradient of zero is imposed both on the sides and bottom of the domain:

$$\begin{aligned} \frac{\partial \Phi^2}{\partial \eta}(x, z_b) &= 0 \\ \frac{\partial \Phi^m}{\partial x}(0, z) = \frac{\partial \Phi^m}{\partial x}(L, z) &= 0 \quad \text{for } m=1,2 \end{aligned} \quad (2)$$

where L is the domain length and η is the direction normal to the bottom boundary. The final boundary condition imposed is a mixed Dirichlet-Neumann condition along the water table, assumed not to intersect the ground surface:

$$\frac{\partial \Phi^1(x, z_1)}{\partial \eta} = R(x) \quad (3a)$$

$$\Phi^1(x, z_1(x)) = k_1 z_1(x) \quad (3b)$$

where $R(x)$ is the specified recharge/discharge distribution. For both of these conditions to be met, the surface location $z_1(x)$ must be identified, the primary goal of the algorithm described in this paper. Note that the solution to the above partial differential equation with these boundary conditions is not unique, so the head is here fixed to a specified value at the intersection of the water table and the left boundary. Also, for global water mass

balance to be conserved without introducing singular behavior at the point of fixed head, the net recharge through the water table is here required to be zero.

The flow solution is assumed to be in the form of a series solution, obtained through the method of separation of variables:

$$\Phi^m(x, z) = \sum_{n=0}^N \cos(\omega_n x) (a_n^m e^{\omega_n z} + b_n^m e^{-\omega_n z}) \quad (4)$$

where N is the number of terms in the series, and a_n^m and b_n^m are the series coefficients associated with the m^{th} layer. Solution of this form satisfy the governing equation (Eq. 1) by definition and satisfy the side no-flow conditions by choosing $\omega_n = \frac{n\pi}{L}$ for all n .

As described by Wong and Craig¹, the coefficients a_n^m and b_n^m can be calculated to satisfy the head and flow continuity conditions across the unconformity and no-flow conditions along the bottom of the modeled domain (Eq. 2). In addition, the Dirichlet condition can here be replaced by the Neumann condition of Eq. (3). For any given guess of $z_1(x)$, here denoted with the superscript r , the series solution coefficients are obtained through minimizing the sum of square errors (SSE) in the continuity and boundary conditions along all of the interfaces at a set of NC control points per interface. This task merely involves the solution of a linear system of equations. The complete system of equations can be found in Wong and Craig¹, with the lone revision of the Neumann boundary condition, such that the SSE from the top boundary becomes:

$$\text{SSE}_1 = \sum_{i=0}^{NC} \left(\left. \frac{\partial \Phi}{\partial \eta} \right|_{(x_i, z_1(x_i))} - R(x_i) \right)^2 \quad (5)$$

4 ITERATIVE ALGORITHM

With the solution approach for any fixed guess of water table elevation $z_1^r(x)$ in hand, an iterative algorithm must used to intelligently update the elevation of the water table. Following Gill and Read⁷, the initial guess for the water table is uniform. The updated water table is found by solving for the coefficients as discussed above, then setting the new surface elevation at all of the control points equal to the head along the water table at the same x location, i.e.,

$$z_1^{r+1}(x_i) = \frac{\Phi^1(x_i, z_1^r(x_i))}{k_1} \quad (6)$$

Where Φ^1 is calculated using Eq. (4) with the most recent coefficient values. Note that the water table need not be explicitly represented by a continuous function; it is sufficient to store only the locations of the control points along the water table surface. Tangents to this surface, as needed for the proper calculation of the system of linear algebraic equations for the next iteration, are calculated using the continuous form of the solution in terms of discharge potential, which is analytically calculable, i.e.,

$$\left. \frac{\partial z_1^{r+1}}{\partial x} \right|_{x_i} = \frac{1}{k_1} \frac{\partial \Phi^1(x_i, z_1^r(x_i))}{\partial x} \quad (7)$$

The water table process is repeatedly updated in this manner until the Dirichlet condition of Eq. (3) is met to an acceptable degree, here considered to be the case when the error in water table elevation (e_{loc}) is below some user-specified tolerance. This error is calculated as:

$$e_{\text{loc}} = \sqrt{\sum_{i=0}^{NC} \left(z_1(x_i) - \frac{\Phi^1(x_i, z_1(x_i))}{k_1} \right)^2} \quad (8)$$

5 ANALYSIS

5.1 Example 1: Various flow nets with different recharge distributions

The groundwater flow solutions are first varied under different arbitrary stratigraphy and recharge distribution functions to illustrate the convergence properties of the algorithm. As shown in Figure 2, the recharge functions are either linear or a combination of trigonometric functions. The conductivities in each scenario are $k_1=1 \text{ md}^{-1}$ and $k_2=5 \text{ md}^{-1}$. The convergence for each of these cases is shown in Figure 3; rapid log-linear convergence is seen in all cases, but varies with problem geometry.

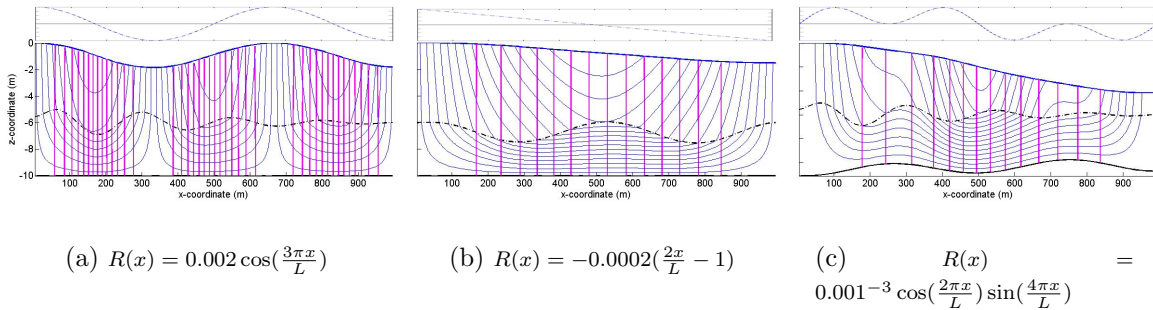


Figure 2: Different recharge functions (top) applied to a 2-layer aquifer system with flow net (bottom). Hydraulic conductivity for each layer is $k_1=1 \text{ md}^{-1}$ and $k_2=5 \text{ md}^{-1}$.

5.2 Example 2: Impact of hydraulic conductivity ratio

As a second example, the hydraulic conductivity ratio is varied ($k_1/k_2=1/5, 1/10,$ and $1/50$) while other characteristics of the aquifer remain the same. As shown in Figure 4, although the flow distributions are similar in all scenarios, the water table becomes flatter as the conductivity ratio (and effective hydraulic conductivity of the entire aquifer system) is decreased. This is consistent with mounding behavior seen in lower-conductivity single-layer unconfined systems, whereby an increase in hydraulic conductivity reduces the steady-state water table gradient.

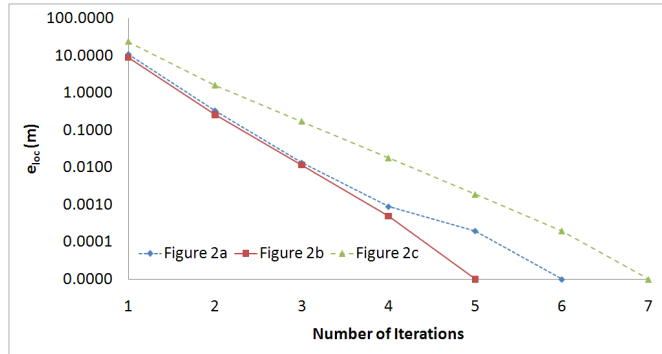


Figure 3: Convergence of the algorithm for the test cases shown in figure ??

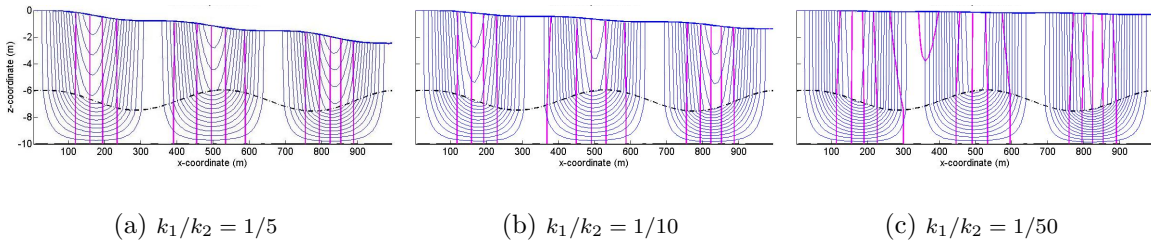


Figure 4: Different water table elevation in a 2-layer aquifer system with $R(x) = 0.002 \cos(3\pi x/L) \sin(3\pi x/L)$.

5.3 Example 3: Impact of arbitrary bottom boundary geometry

In the third example (shown in Figure 5), the aquifer system has a non-uniform bottom boundary and the conductivity ratio between the two layers is fixed at 1 : 5. As listed in Table 1, the absolute value of both head and flow errors are on the magnitude of 10^{-5} m and 10^{-5} md⁻¹, respectively. One interesting feature of these solutions is that the water table dips sharply where there is both extraction (i.e., $R(x) < 0$) and a shallow aquifer base, as can be seen in Figures 5(a), 5(c), and (to a lesser extent) 5(e).

6 CONCLUSIONS

The results of the simulations run with series solution method show that three controlling factors: the recharge distribution, the conductivity ratio, and the elevation of a bottom boundary, all have certain degree of influence on the free water table. The iterative algorithm developed here was shown to be quite efficient and accurate; convergence was log-linear and errors were on the order of 10^{-5} m . Future extensions include mixed boundary conditions where the water table (still treated using the free boundary condition) can intersect both the unconformities and topographic surface.

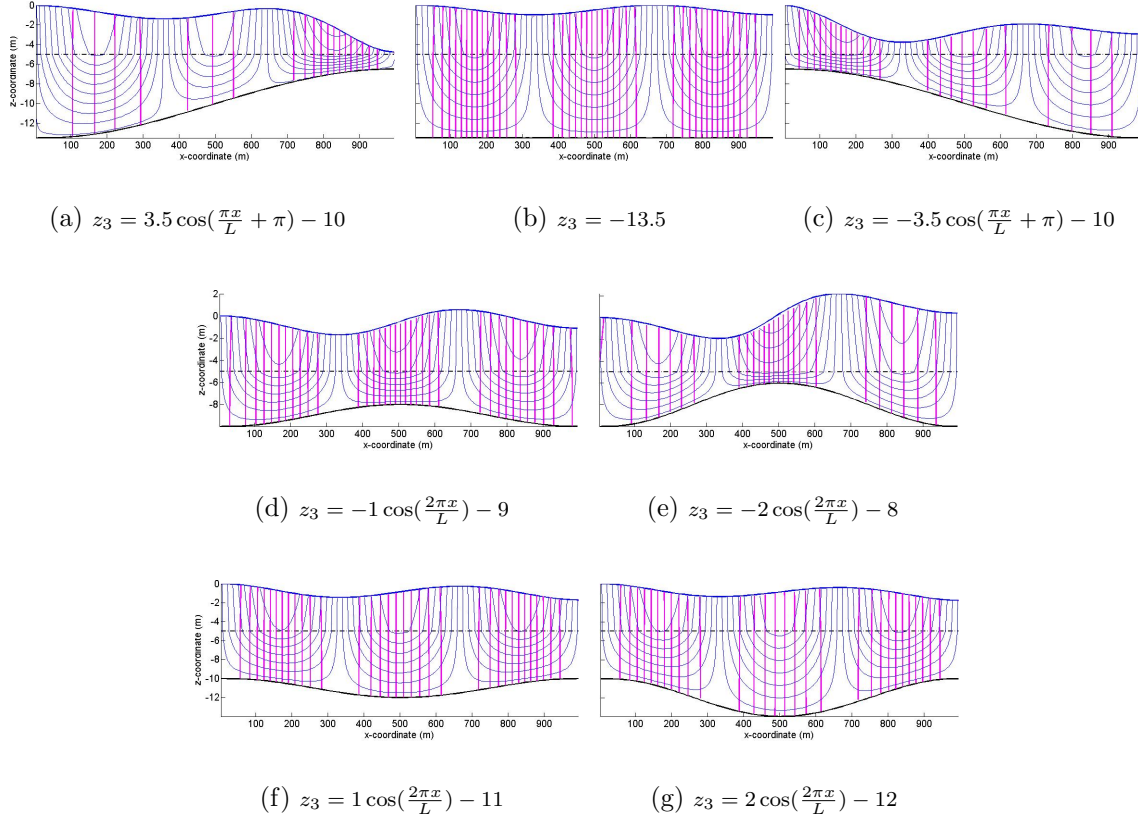


Figure 5: Groundwater flow distribution due to various bottom boundary, with $R(x) = 0.001 \cos(2\pi x/L) \sin(4\pi x/L)$, and $k_1=1 \text{ md}^{-1}$ and $k_2=5 \text{ md}^{-1}$.

REFERENCES

- [1] S. Wong and J.R. Craig. Series solutions for flow in stratified aquifers with natural geometry. *Advances in Water Resources*, **33**, 48-54, (2010).
- [2] J.A. Tóth. A theoretical analysis of groundwater flows in small drainage basins. *Journal of Geophysical Research*, **68**, 4795-4812, (1963).
- [3] R.A. Freeze and P.A. Witherspoon. A theoretical analysis of groundwater flows in small drainage basins. *Water Resources Research*, **2**, 641-656, (1966).
- [4] W.W. Read. Series solution for Laplace's equation with nonhomogeneous mixed boundary conditions and irregular boundaries. *Mathematical and Computer Modelling*, **17**, 9-19, (1993).
- [5] W.W. Read. Errata to Series solution for Laplace's equation with nonhomogeneous mixed boundary conditions and irregular boundaries. *Mathematical and Computer Modelling*, **18**, 107, (1993).

Table 1: Absolute continuity and boundary errors across at each z_m in the 2-layer aquifer. Errors are calculated at the control points.

Figure 5		head(m)		flow(md ⁻¹)	
	z_m	max	min	max	min
a	z_1	N/A	N/A	1.15E-05	-1.04E-05
	z_2	3.28E-07	-3.32E-07	1.72E-07	-2.68E-07
	z_b	N/A	N/A	7.56E-07	-8.83E-07
b	z_1	N/A	N/A	9.81E-09	-8.71E-09
	z_2	7.33E-11	-7.49E-11	6.23E-11	-3.94E-11
	z_b	N/A	N/A	2.10E-11	-1.01E-11
c	z_1	N/A	N/A	6.99E-06	-6.34E-06
	z_2	4.19E-07	-4.19E-07	3.29E-07	-2.97E-07
	z_b	N/A	N/A	1.70E-06	-1.63E-06
d	z_1	N/A	N/A	6.44E-08	-5.79E-08
	z_2	8.74E-10	-8.81E-10	5.67E-10	-5.78E-10
	z_b	N/A	N/A	1.83E-09	-1.81E-09
e	z_1	N/A	N/A	2.41E-07	-2.16E-07
	z_2	4.16E-09	-4.06E-09	7.31E-09	-7.16E-09
	z_b	N/A	N/A	1.79E-08	-1.75E-08
f	z_1	N/A	N/A	3.84E-08	-3.46E-08
	z_2	4.09E-10	-4.97E-10	3.31E-10	-2.65E-10
	z_b	N/A	N/A	8.86E-10	-9.05E-10
g	z_1	N/A	N/A	3.14E-08	-2.82E-08
	z_2	4.05E-10	-4.13E-10	2.17E-10	-2.47E-10
	z_b	N/A	N/A	1.57E-09	-1.70E-09

- [6] W.W. Read. A comparison of analytic series method for Laplacian free boundary problems. *Mathematical and Computer Modelling*, **20**, 31-44, (1994).
- [7] Gill, A. W., W.W. Read. Efficient analytic series solutions for two-dimensional potential flow problems. *International Journal for Numerical Methods in Fluids*, **23**, 415-430, (1996).
- [8] W.W. Read and R.E. Volker. A comparison of analytic series method for Laplacian free boundary problems. *Computational Techniques and Applications'89*, 707-714, (1990).
- [9] P. Tritscher, W.W. Read, P. Broadbridge, and J.M. Stewart. Steady infiltration in sloping porous domains: the onset of saturation. *Transport in Porous Media*, **31**, 1-17, (1998).
- [10] J.R. Craig. Analytical solutions for 2D topography-driven flow in stratified and syncline aquifers. *Advances in Water Resources*, **31**, 1066-1073, (2008).